Excitotoxicity and Overnutrition Additively Impair Metabolic Function and Identity of Pancreatic β-Cells

Anna B. Osipovich,[1,2] Jennifer S. Stancill,[2,3] Jean-Philippe Cartailler,[2] Karrie D. Dudek,[2,3] and Mark A. Magnuson[1,2,3]

Diabetes 2020;69:1476–1491 | https://doi.org/10.2337/db19-1145

A sustained increase in intracellular Ca^{2+} concentration (referred to hereafter as excitotoxicity), brought on by chronic metabolic stress, may contribute to pancreatic β-cell failure. To determine the additive effects of excitotoxicity and overnutrition on β-cell function and gene expression, we analyzed the impact of a high-fat diet (HFD) on *Abcc8* knockout mice. Excitotoxicity caused β-cells to be more susceptible to HFD-induced impairment of glucose homeostasis, and these effects were mitigated by verapamil, a Ca^{2+} channel blocker. Excitotoxicity, overnutrition, and the combination of both stresses caused similar but distinct alterations in the β-cell transcriptome, including additive increases in genes associated with mitochondrial energy metabolism, fatty acid β-oxidation, and mitochondrial biogenesis and their key regulator *Ppargc1a*. Overnutrition worsened excitotoxicity-induced mitochondrial dysfunction, increasing metabolic inflexibility and mitochondrial damage. In addition, excitotoxicity and overnutrition, individually and together, impaired both β-cell function and identity by reducing expression of genes important for insulin secretion, cell polarity, cell junction, cilia, cytoskeleton, vesicular trafficking, and regulation of β-cell epigenetic and transcriptional program. Sex had an impact on all β-cell responses, with male animals exhibiting greater metabolic stress-induced impairments than females. Together, these findings indicate that a sustained increase in intracellular Ca^{2+}, by altering mitochondrial function and impairing β-cell identity, augments overnutrition-induced β-cell failure.

The loss of β-mass and function in response to metabolic stress is a major determinant of type 2 diabetes (T2D) (1). While multiple mechanisms, including glucolipotoxicity, excitotoxicity, inflammation, endoplasmic reticulum (ER) stress, and oxidative stress (2–5), have been implicated in metabolic stress–induced β-cell failure, the molecular and cellular mechanisms that actually cause the loss of β-cell function and development of T2D are not understood.

Excitotoxicity refers to the pathological process in excitable cells in which overstimulation leads to a sustained increase in intracellular Ca^{2+} concentration ($[Ca^{2+}]_i$), resulting in disrupted homeostasis, loss of cell function, or cell death (6). In pancreatic β-cells, metabolic stress–induced increases in $[Ca^{2+}]_i$ activate Ca^{2+}/calmodulin-dependent kinases (CaMKs), calcineurin (a Ca^{2+}-dependent phosphatase), and other Ca^{2+}-dependent proteins, causing alterations in β-cell gene expression that negatively impact both β-cell mass and function (7). Increases in $[Ca^{2+}]_i$ have been described in rat islets cultured in high glucose (8), in mouse islets from obese (*db/db*) mice (9), in islets of mice fed a high-fat diet (HFD) (10), and in β-cells that exhibit chronic membrane depolarization (11). Both the verapamil-induced blockage of Ca^{2+} influx (12) and genetic knockdown of Cavβ3, a Ca^{2+} channel subunit (13), by reducing $[Ca^{2+}]_i$, attenuate β-cell loss and diabetes in animal models, suggesting that an increase in $[Ca^{2+}]_i$ is a fundamental determinant of stress-induced β-cell failure.

Overnutrition, by elevating circulating free fatty acids (FFAs), contributes to insulin resistance, increasing insulin biosynthesis and secretion (14). The prolonged exposure of β-cells to FFAs elicits multiple responses, including the activation of ER stress, oxidative stress, and inflammatory signaling pathways (15,16). Most notably, FFA-induced oxidative stress triggers the release of Ca^{2+} from ER stores, increasing $[Ca^{2+}]_i$, accentuating ER stress, and inducing apoptosis (17).

[1]Department of Molecular Physiology and Biophysics, Vanderbilt University, Nashville, TN
[2]Vanderbilt Center for Stem Cell Biology, Vanderbilt University, Nashville, TN
[3]Department of Cell and Developmental Biology, Vanderbilt University, Nashville, TN

Corresponding author: Mark A. Magnuson, mark.magnuson@vanderbilt.edu

Received 15 November 2019 and accepted 20 April 2020

This article contains supplementary material online at https://doi.org/10.2337/figshare.12170184.

Sex also influences the response of β-cells to stress (18). Women are less likely than men to develop T2D and require a higher BMI to do so (19). Increased estrogen receptor signaling (20), sex-specific differences in islet DNA methylation status (21), and differences in the expression of islet-enriched transcription factors (TFs) and genes involved in cell cycle regulation (22) have all been suggested as causes for these differences.

To obtain a systems-wide understanding of the effects of both excitotoxicity and overnutrition on β-cell function and gene expression, we used mice lacking *Abcc8*, a critical subunit of the ATP-dependent K^+ channel (K_{ATP}). Previously, we have shown that β-cells from these mice exhibit chronic membrane depolarization and increases in $[Ca^{2+}]_i$ that cause impairments in islet morphology, glucose tolerance, and β-cell identity (11,23). Because the loss of β-cell function in mice lacking *Abcc8* develops slowly over several months (23), the individual and combined effects of excitotoxicity and overnutrition on β-cell function and gene expression were determined prior to the onset of hyperglycemia and glucotoxicity (11). Additionally, by using a recently described *Ins2*^{Apple} allele, we avoided confounding effects of the MIP-GFP transgene (22).

RESEARCH DESIGN AND METHODS

Mouse Lines and Husbandry

The *Abcc8*$^{tm1.1Mgn}$ (23) and *Ins2*^{Apple} (22) alleles were bred into and maintained as C57BL/6J congenic lines (stock 000664; The Jackson Laboratory). At weaning (3–4 weeks of age), mice were fed either regular chow (RC) (4.5% fat content) (5L0D; PicoLab) or HFD (60% fat content) (D12492; Research Diets, Inc.) for 5 weeks. Verapamil (1 mg/mL) (V4629; Sigma-Aldrich) was administered through the drinking water during the period of HFD feeding. All animal experimentation was performed under the oversight of the Vanderbilt University Institutional Animal Care and Use Committee.

Glucose Homeostasis

Intraperitoneal glucose tolerance tests (GTTs) were performed following a 16-h overnight fast. Blood glucose concentrations were measured at 0, 15, 30, 60, and 120 min after administering D-glucose (2 mg/g body mass). Insulin tolerance testing was performed following a 4-h morning fast by administering 0.1 units/mL insulin (in Dulbecco's PBS) (Humulin R; Eli Lilly and Company) and measuring blood glucose concentrations at 0, 15, 30, 60, and 120 min.

Islet Isolation and Culture

Islets were isolated following injection of 0.6 mg/mL Collagenase P (Roche) into the pancreatic bile duct followed by Histopaque-1077 (Sigma-Aldrich) fractionation and handpicking. For FACS and RNA sequencing, islets from two to four mice were pooled for each sample. Islets were cultured in low-glucose DMEM (11966–025; Gibco) containing 1 g/L glucose and supplemented with 10% FBS and penicillin/streptomycin (100 mg/mL) (Gibco) at 37°C with 5% CO_2 infusion and 95% humidity. Palmitic acid (PA) (P0500; Sigma-Aldrich) was diluted in 50% ethanol to 100 mmol/L and conjugated to an FA-free BSA (A6003; Sigma-Aldrich) to generate a 5 mmol/L PA/5% FA-free BSA stock solution. Experimental media concentrations of the compounds used were 100 μmol/L for tolbutamide (T0891; Sigma-Aldrich), 0.5 mmol/L for PA, and 50 μmol/L for verapamil (V4629; Sigma-Aldrich).

β-Cell Isolation, RNA Isolation, and Quantitative PCR

Purified β-cells were obtained as previously described (15) in which live cells expressing red fluorescence were sorted with a 100-μm nozzle using the FACSAria II instrument (BD Biosciences). Cells were collected in chilled Homogenization Solution from the Maxwell 16 LEV simplyRNA Tissue Kit (TM351; Promega), and RNA was isolated as directed. For quantitative PCR (qPCR), reverse transcription was done using a High-Capacity cDNA Reverse Transcription Kit (Thermo Fisher Scientific). A total of 2 ng cDNA was used in real-time qPCR with Power SYBR Green PCR Master Mix (Thermo Fisher Scientific) using a CFX96 Real-Time PCR system (Bio-Rad Laboratories). Primers are listed in Supplementary Table 1.

RNA Sequencing and Data Analysis

RNA samples were analyzed using an Agilent 2100 Bioanalyzer, and only those samples with an RNA integrity number of seven or above were used. cDNA synthesis and amplification were performed using the SMART-Seq v4 Ultra Low Input RNA Kit for Sequencing (Takara Bio, Inc.) using 10 cycles of PCR. cDNA libraries were constructed using the Low Input Library Prep Kit (Takara Bio, Inc.). An Illumina NovaSeq 6000 instrument was used to produce paired-end, 150-nucleotide reads for each RNA sample. Paired-end sequencing of 31 samples produced ~1.55 billion raw sequencing reads. The Spliced Transcripts Alignment to a Reference (STAR) application (16) was used to perform sequence alignments to the mm10 (GRCm38) mouse genome reference and GENCODE comprehensive gene annotations (release M17). Overall, 80–88% of the raw sequencing reads were uniquely mapped to genomic sites, resulting in 1.3 billion usable reads. HTSeq was used for counting reads mapped to genomic features (17), and DESeq2 was used for differential gene expression analysis (18). $P_{adj} < 0.05$ cutoff was used to define differentially expressed genes. Gene ontology (GO) analysis of differentially expressed genes was performed using Metascape (19).

Mitochondrial Respirometry and mtDNA Copy Number

Oxygen consumption rates (OCRs) of isolated islets were determined using a Seahorse XF96 respirometer (Agilent Technologies), as described (24). A total of 10–20 islets/well were loaded onto a Cell-Tak (Corning) precoated XF96 spheroid plate (Agilent Technologies) and preincubated for 2 h at 37°C without CO_2 in a Seahorse assay DMEM (Agilent Technologies) supplemented with 3 mmol/L

glucose, 1 mmol/L pyruvate, and 2 mmol/L glutamine. After measuring basal OCR, glucose (20 mmol/L), oligomycin (5 mmol/L), carbonyl cyanide-4-(trifluoromethoxy)phenylhydrazone (FCCP) (1 mmol/L), or antimycin A/rotenone (2.5 mmol/L) was added at indicated time points to modulate mitochondrial OCR response. For mtDNA copy number measurements, islet DNA was isolated with a DNeasy kit (Qiagen) and analyzed by qPCR with primers for mtDNA-encoded gene *mt-CO1* and nuclear gene *Ndufv1*. Relative copy number was calculated as 2^([Ct(mtDNA) * E] − [Ct(nuclear DNA) * E]), where E is efficiency of corresponding qPCR determined from standard curves and Ct is threshold cycle.

Data and Resource Availability

RNA-sequencing data are available in ArrayExpress (https://www.ebi.ac.uk/arrayexpress) under accession number E-MTAB-8643.

RESULTS

Excitotoxicity and Overnutrition Additively Impair Glucose Tolerance

To compare the effects of excitotoxicity and overnutrition on pancreatic β-cells, we fed C57BL/6J (wild-type [WT]) and *Abcc8* knockout (KO) mice either RC or HFD for 5 weeks. Both groups contained male and female animals ($n = 7–8$ of each sex), and all animals gained weight on HFD (Fig. 1*A*). Blood glucose measurements after 5 weeks showed that the KO animals had lower fasting blood glucose in comparison with WT mice (Fig. 1*B*), consistent with previous observations that *Abcc8* KO mice have impaired glucagon secretion (25). In contrast, fed blood glucose levels were higher in the HFD-KO mice compared with the RC-KO and HFD-WT animals (Fig. 1*C*). Treatment with verapamil, a Ca^{2+} channel blocker, during HFD lowered the fed blood glucose concentration in both the HFD-KO and HFD-WT mice (Fig. 1*C*).

After 5 weeks, HFD-KO mice exhibited greater glucose intolerance compared with the RC-KO, RC-WT, and HFD-WT mice (Fig. 1*D* and *F*). Verapamil treatment improved glucose tolerance in the HFD-WT mice, while in HFD-KO mice, the effect of the drug was apparent only at 120 min after glucose administration (Fig. 1*E* and *F*). Both the RC-KO and HFD-KO animals had increased insulin sensitivity compared with the RC-WT and HFD-WT mice, respectively (Supplementary Fig. 1*A* and *C*). However, while verapamil increased insulin sensitivity of HFD-WT compared with the RC-WT mice, it had no effect on the HFD-KO mice (Supplementary Fig. 1*B* and *C*). These findings indicate that *Abcc8* KO mice are more insulin sensitive, have a higher fed blood glucose concentration, and are more intolerant of glucose on an HFD than are WT animals. Interestingly, coadministration of verapamil during HFD feeding normalized blood glucose concentration in the KO animals independent of improvements in insulin sensitivity. Together, these findings indicate that excitotoxicity increases the susceptibility of β-cells to the negative effects of overnutrition.

Effects of Excitotoxicity and Overnutrition on β-Cell Gene Expression

To determine how excitotoxicity, overnutrition, and both stresses affect gene expression, we performed RNA sequencing on FACS-purified β-cells. All mice were identical in strain (C57BL/6J) and age (8–9 weeks old), but differed by sex, the presence or absence of *Abcc8*, and diet (RC vs. HFD). Sample clustering by principal component analyses of data from 31 samples (Supplementary Table 2) showed clear separation of WT and KO samples and indicated that the effect of the *Abcc8* KO was much greater than that of the HFD (Supplementary Fig. 2). After pooling the data from both sexes, we performed three differential expression (DE) analyses, as summarized in Supplementary Table 3.

Excitotoxicity

To determine effects of excitotoxicity, we first compared the RC-KO and RC-WT data sets. Similar to our previous report, which used an MIP-GFP transgene (11), we observed a profound alteration in the β-cell transcriptome with a total of 7,393 genes being affected (3,957 upregulated genes [URGs] and 3,436 downregulated genes [DRGs]) (Fig. 2*A* and *B* and Supplementary Table 4). The magnitude of gene dysregulation was similar to our prior study ($R = 0.72$) (Supplementary Fig. 3) with differences in dysregulated gene sets attributed to leaky growth hormone from the MIP-GFP transgene (22).

GO term and pathway enrichment analysis of protein coding URGs and DRGs revealed that the URGs were enriched in mitochondrial genes involved in oxidative phosphorylation, mitochondrial organization, multiple metabolic pathways, and lysosomal genes (Fig. 2*C* and Supplementary Table 5). In contrast, DRGs were associated with microtubule cytoskeleton, insulin secretion, chromatin organization, transcription, *FoxO* and *Mapk* signaling, and cell junction organization. Several of the top URGs are critical for neural and β-cell development, including TFs (*Ascl1*, *Fev*, and *Neurog3*) and growth factors (*Nog*, *Wif1*, and *Igf2*) (Fig. 2*D*). Other top URGs include gastrin (*Gast*), a putative marker of dedifferentiating β-cells (26), the EF-hand domain Ca^{2+}-binding protein *S100a6*, voltage-gated K^+ channels (*Kcnc2* and *Kcns3*), and Ca^{2+} channels (*Slc24a33* and *Cacng3*), which are likely involved in compensatory regulation of ion flow in the absence of functional K_{ATP} channels (Fig. 2*D*). Top DRGs are involved in insulin secretion (*Nnat* and *Ins1*), cell junction formation (*Cldn8* and *Pcdh15*), potassium ion transport (*Trpm5* and *Hcn1*), response to vascular endothelial growth factor (*Kdr* and *Flt1*), and gene transcription *(Npas4* and *Egr4*). These results indicate that β-cell excitotoxicity increases expression of many developmentally important TFs and genes required for mitochondrial energy production while also broadly downregulating genes involved in insulin secretion, chromatin maintenance, and cytoskeletal function.

Overnutrition

Next, we determined the effects of overnutrition on WT β-cells by comparing the HFD-WT and RC-WT data sets.

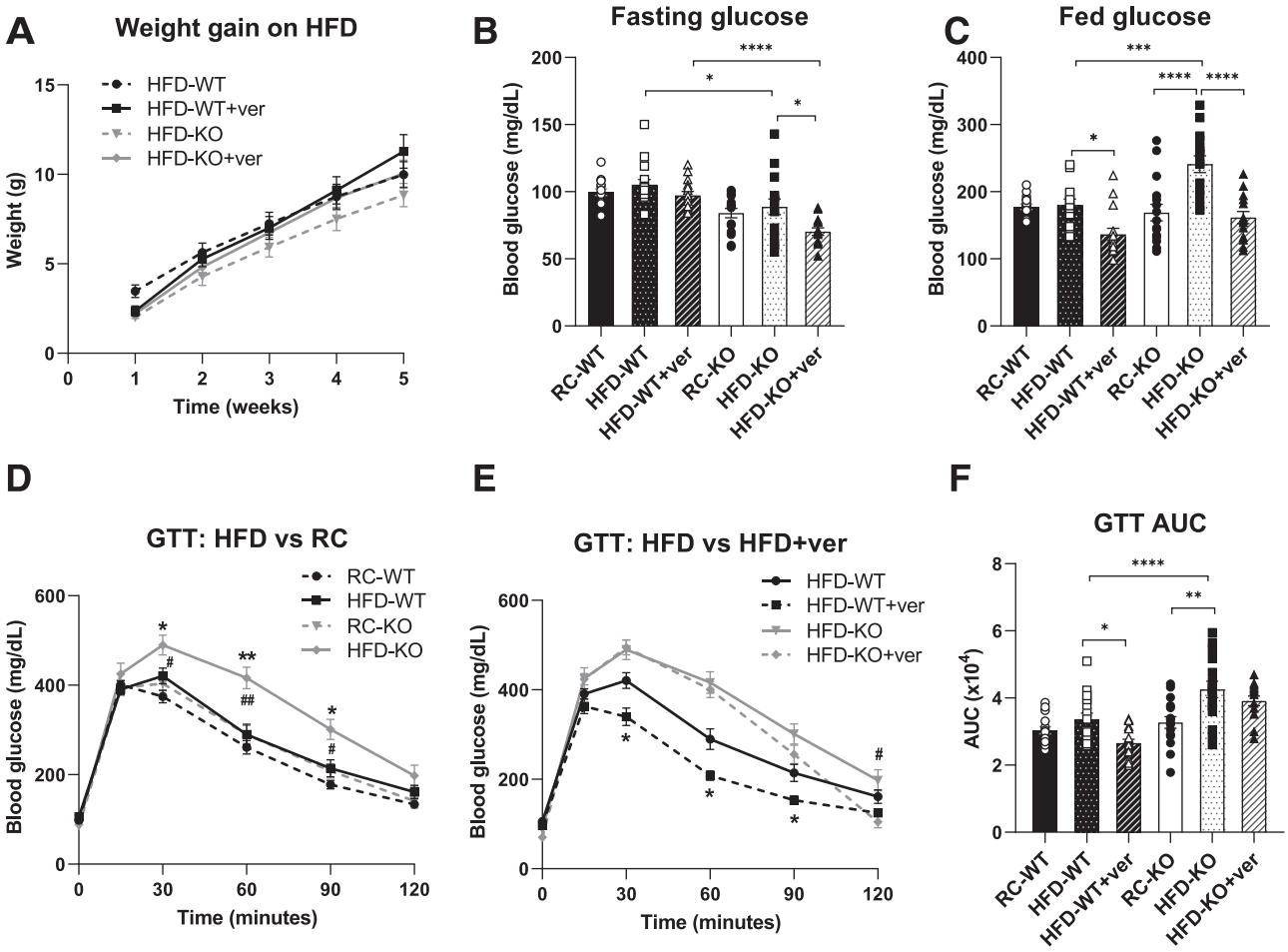

Figure 1—*Abcc8* KO mice exhibit impaired β-cell function after 5 weeks on HFD that is improved with the addition of verapamil. *A*: Weight gain on HFD for 5 weeks was similar for both WT and *Abcc8* KO animals. Fasting (*B*) and fed (*C*) blood glucose measurements for RC- and HFD-fed mice at 8–9 weeks. KO mice have lower fasting blood glucose than WT mice. Fed blood glucose is elevated in HFD-KO and is lowered with the addition of verapamil (+ver). *D*: Intraperitoneal GTT results comparing RC- and HFD-fed mice at 8–9 weeks. HFD-KO mice have impaired glucose tolerance in comparison with WT and RC-KO mice. *$P \leq 0.05$, **$P \leq 0.01$: HFD-WT vs. HFD-KO; #$P \leq 0.05$, ##$P \leq 0.01$: HFD-KO vs. RC-KO. *E*: GTT results comparing HFD- and HFD+ver–fed mice at 8–9 weeks. $n = 14–16$. *$P \leq 0.05$: HFD-WT vs. HFD-WT+ver; #$P \leq 0.05$: HFD-KO vs. HFD-KO+ver. *F*: GTT area under the curve (AUC) measurements. Addition of verapamil improves glucose tolerance of HFD-WT and HFD-KO mice. $n = 14–16$ (7–8 males and 7–8 females) for each condition. Error bars: ± SEM. *$P \leq 0.05$; **$P \leq 0.01$; ****$P \leq 0.0001$ (determined by ANOVA).

This analysis revealed 2,372 affected genes (1,320 URGs and 1,052 DRGs) (Fig. 3*A* and *B* and Supplementary Table 4). Functional enrichment analysis indicated that URGs were involved in ER protein processing, ER stress, unfolded protein responses, glycan biosynthesis, and cell cycle regulation. In contrast, DRGs were involved in chromatin organization and response to hormone stimulus, as well as mammalian target of rapamycin signaling pathways (Fig. 3*C* and Supplementary Table 5). The top URGs included hormone receptors (*Ptger3* and *Oxtr*), immune cell surface proteins (*Cd74* and *H2-Eb2*), and cell cycle regulators (*Cdc20* and *Ccnb1*) (Fig. 3*D*). Top DRGs included receptors (*Erbb2* and *Hspg2*), extracellular matrix proteins (*Olfm2* and *Hspg2*), secreted growth factors (*Igfbp5* and *Angptl7*), and TFs (*Trnp1* and *Epas1*). These results indicate that overnutrition causes increased expression of genes involved in ER protein processing and β-cell proliferation and downregulation of genes involved in mammalian target of rapamycin signaling and chromatin maintenance.

Excitotoxicity and Overnutrition

To determine the combined effects of excitotoxicity and overnutrition, we compared the HFD-KO and RC-WT data sets and identified 8,836 dysregulated genes (4,322 URGs and 4,514 DRGs) (Fig. 4*A* and *B* and Supplementary Table 4). URGs were involved in oxidative phosphorylation, the citric acid cycle, and nucleotide metabolism, whereas DRGs were involved in cytoskeleton, insulin secretion, cell projection and cell junction organization, and chromatin and transcriptional regulation (Fig. 4*C* and Supplementary Table 5). Many of the top URGs were also increased in the RC-KO (*Ascl1* and *Stc2*) and HFD-WT (*Cd74* and *Cdc20*) mice (Fig. 4*D*). Interestingly, genes involved in lipid uptake (*Fabp3* and *Apoe*), stimulation of ketogenesis,

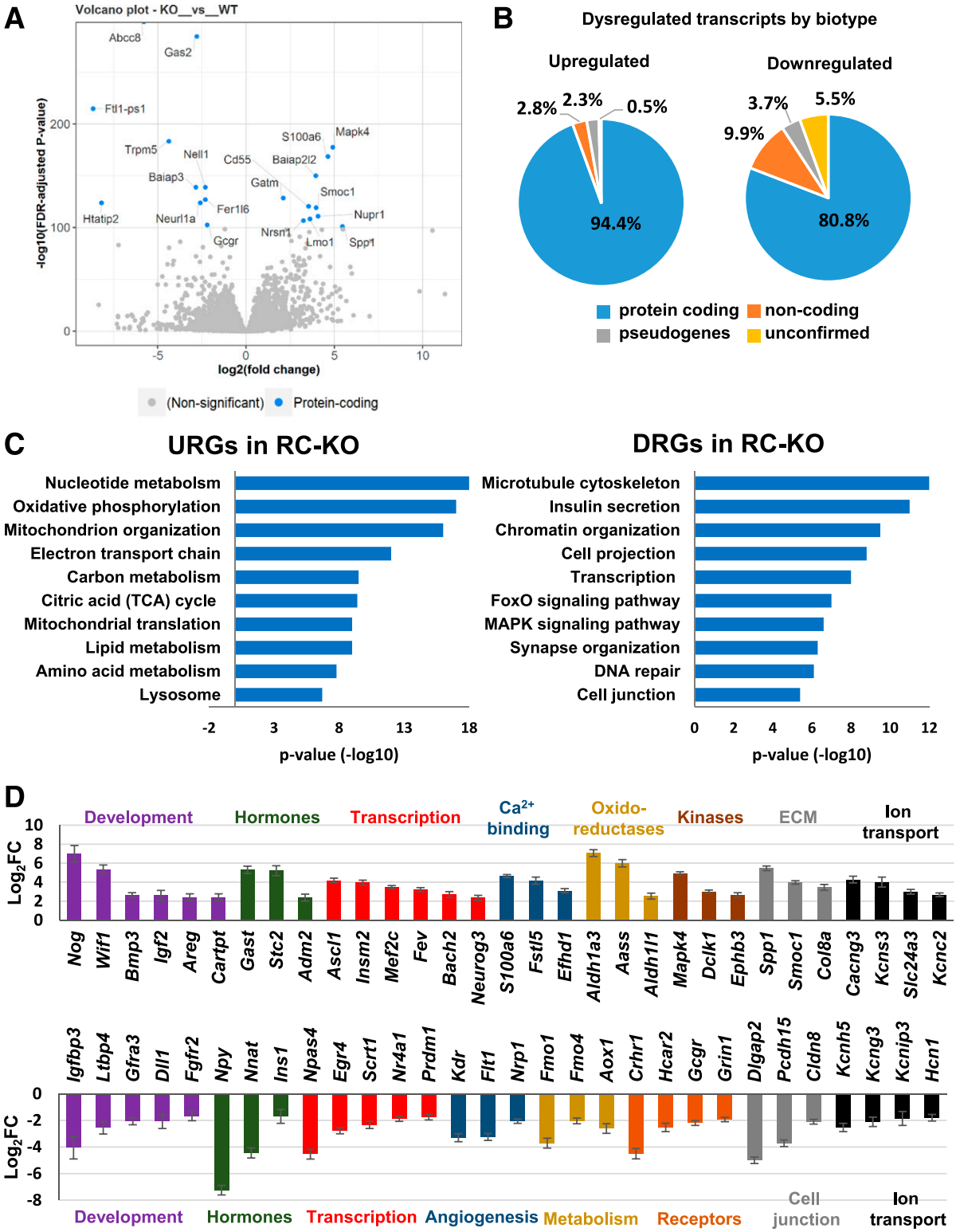

Figure 2—β-Cell transcriptome changes in response to excitotoxicity in *Abcc8* KO mice. *A*: Volcano plot showing distribution of differentially expressed genes (Log_2FC over *P* value) in the RC-KO vs. RC-WT RNA-sequencing comparison. Top 10 differentially expressed genes are indicated by names, and total numbers of URGs and DRGs are shown ($P_{adj} < 0.05$). *B*: Distribution of dysregulated genes by biotype. *C*: Functional enrichment analysis of URGs and DRGs. Select top enriched pathways are shown. *D*: DE levels of select top URGs (top) and DRGs (bottom), with colors indicating gene functional associations. ECM, extracellular matrix; FDR, false discovery rate; Log_2FC, log_2 fold change of gene expression values in normalized counts in RC-KO vs. RC-WT comparison; TCA, tricarboxylic acid.

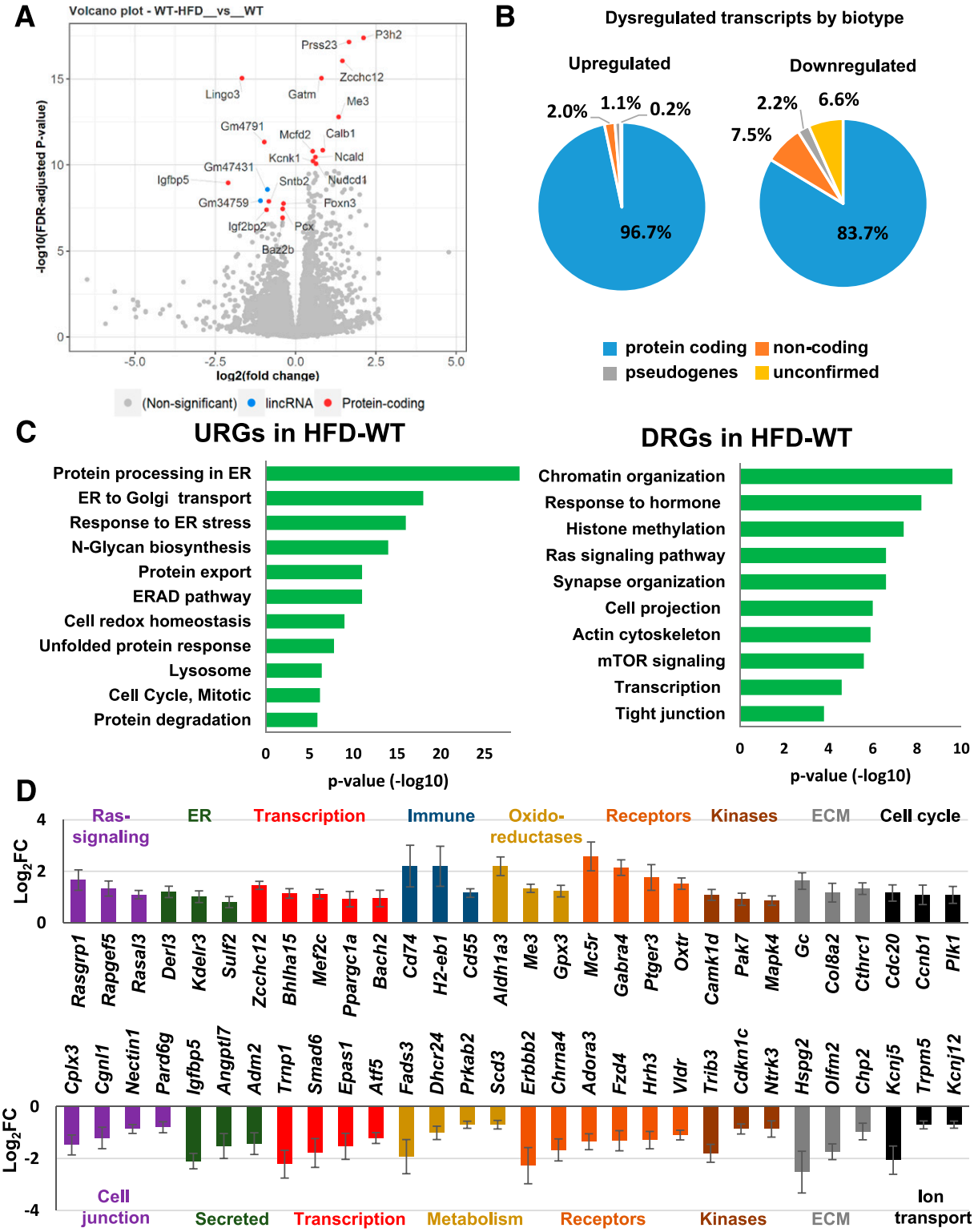

Figure 3—β-Cell transcriptome changes in response to overnutrition (HFD) in WT mice. *A*: Volcano plot showing distribution of differentially expressed genes (Log_2FC over *P* value) in HFD-WT vs. RC-WT RNA-sequencing comparison. Top 10 differentially expressed genes are indicated by names, and total numbers of URGs and DRGs are provided ($P_{adj} < 0.05$). *B*: Distribution of dysregulated genes by biotype. *C*: Functional enrichment analysis of URGs and DRGs. Select top enriched pathways are shown. *D*: DE levels of select top URGs (top) and DRGs (bottom), with colors indicating gene functional associations. ECM, extracellular matrix; ERAD, ER-associated protein degradation; FDR, false discovery rate; Log_2FC, log_2 fold change of normalized gene expression between HFD-WT and RC-WT samples; mTOR, mammalian target of rapamycin.

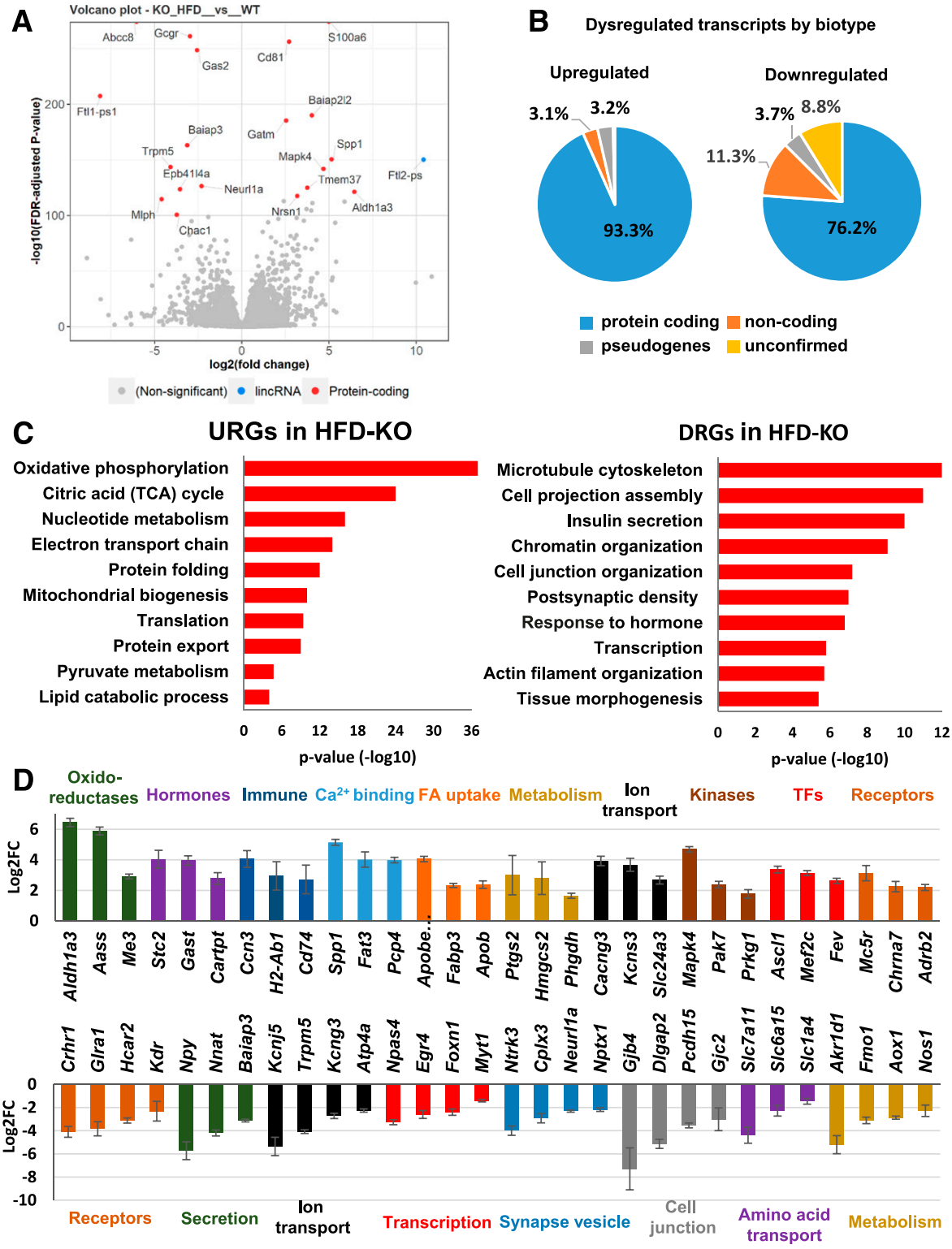

Figure 4—β-Cell transcriptome changes in response to excitotoxicity and overnutrition (HFD) in *Abcc8* KO mice. *A*: Volcano plot showing distribution of differentially expressed genes (Log_2FC over *P* value) in HFD-KO vs. RC-WT RNA-sequencing comparison. Top 10 differentially expressed genes are indicated by names, and total numbers of URGs and DRGs are provided ($P_{adj} < 0.05$). *B*: Distribution of dysregulated genes by biotype. *C*: Functional enrichment analysis of URGs and DRGs. Select top enriched pathways are shown. *D*: DE of select top URGs (top) and DRGs (bottom). Colors indicate gene functional associations. FDR, false discovery rate; Log_2FC, log_2 fold change HFD-KO vs. RC-WT; TCA, tricarboxylic acid.

and impairment of glycolysis (*Hmgcs2* and *Pdk4*) were only upregulated in response to the combined stresses. The top DRGs included genes involved in cell adhesion (*Gjd4* and *Dlagap2*), acid transporters (*Slc28a2* and *Slc7a11*), and many genes that were also downregulated in either RC-KO (*Npy* and *Nnat*) or HFD-WT (*Igfpb5* and *Atf5*) mice. These findings indicate that the combination of excitotoxicity and overnutrition causes a further increase in the expression of β-cell genes involved in energy metabolism and ATP production, as well as genes linked to a decrease in glucose and an increase in FA-derived ketone utilization as an energy source. At the same time, genes associated with cytoskeleton and cell junction organization are downregulated.

Excitotoxicity and Overnutrition Affects Many of the Same Genes and Pathways

To better categorize the many different transcriptional responses, we performed a meta-analysis of genes dysregulated in three comparisons (Fig. 5*A*). Major functional categories shared among URGs included oxidative phosphorylation, mitochondrial organization, metabolic pathways, and oxidative stress response, and shared downregulated pathways were chromatin organization, cytoskeleton and cell organization, and DNA damage response (Fig. 5*B* and *C*). The large overlap in genes dysregulated in response to both excitotoxicity and overnutrition (Fig. 6*A*) suggests that Ca^{2+}-mediated nuclear responses are involved in many of the responses of β-cells to overnutrition. Of the 620 URGs that were similarly affected by excitotoxicity (RC-KO vs. RC-WT), overnutrition (HFD-WT vs. RC-WT), or excitotoxicity and overnutrition (HFD-KO vs. RC-WT), the most highly affected genes were *Mc5r*, a melanocortin receptor, *Aldh1a3*, an oxidoreductase for which expression correlates with β-cell failure (27), and *Gabra4*, a GABA receptor subunit that potentiates insulin secretion (28). In contrast, 522 DRGs were shared among all three comparisons with *Trnp1*, a regulator of cell cycle progression (29), tribbles pseudokinase 3 (*Trib3*), a multifunctional signaling protein involved in coordinating stress-adaptive metabolic responses (30), and glucagon receptor (*Gcgr*) being the most highly downregulated.

Functional gene enrichment analysis showed that overlapping stress URGs are involved in ER protein processing, glycan biosynthesis, metabolic pathways, oxidative phosphorylation, and lysosomes (Fig. 6*B* and Supplementary Table 5). Included were genes involved in carbohydrate metabolism (*Me3* and *Mdh1*), amino acid metabolism (*Gatm* and *Oat*), FA β-oxidation (*Acad11* and *Acadvl*), components of complexes I–V of mitochondrial electron transport chain (*Uqcrfs1*, *Atp5d*, *Cox6b1*, and *Ndufc2*), and mitochondrial rRNA proteins (*Mrps12* and*Mrpl51*) (Supplementary Fig. 4). Common URGs also include oxidoreductases (*Ald1a3* and *Aass*), secreted proteins (Gc and *Vgf*), redox homeostasis maintenance genes (*Gsto2* and *Gpx3*), lysosome (*Ctsh* and *Dapl1*), ER protein folding (*Ppib* and *Selenos*), and vesicle traffic (*Rgs8*) genes. Notably, genes involved in Ca^{2+} signaling (*Camk1d* and *Mapkapk3*) and TFs that are activated by Ca^{2+} signaling (*Mef1c* and *Nfatc1*) are among common URGs (Supplementary Fig. 4). Other upregulated TFs include *Fev*, *Bach2, Etv1*, *Ppargc1a*, and *Bhlha15*. Overlapping stress-induced URGs also contain genes involved in DNA damage cell-cycle checkpoint (*Check1* and *Ccng1*), apoptosis regulation (*Bcl2* and *Endog*), potassium ion transport (*Kcnk13* and *Slc12a2*), receptors (*Gabra4* and *Gfra4*), extracellular matrix (*Col8a2* and *P3h2*), and immune response (*H2-Eb1* and *Tnfrsf11b*).

DRGs common to all three comparisons are involved in transcription, chromatin modification, protein phosphorylation, as well as adherens junctions and *FoxO1* signaling pathways (Fig. 6*B* and Supplementary Table 5). Downregulated TFs included known regulators of β-cell identity and function (*Myt1*, *Thra*, *Myt1l*, and *Stat5a*) and many for which the role in β-cells has not been studied (*Mesp2*, *Phf21b*, *Otub2*, and *Chd7*) (Supplementary Fig. 5). Over 40 proteins involved in epigenetic regulation were decreased, including chromatin-modifying enzymes (*Kdm6b*, *Jmjd1c*, and *Kat2b*), DNA methylation enzymes (*Dnmt3a* and *Tet3*), and miRNA-processing proteins (*Ago1* and *Tnrc6c*). Common DRGs also included those involved in regulation of circadian rhythms (*Prkab, Prkag2*, and *Nr1d1*), the DNA damage response (*Plk3*, *Taok1*, and *Primpol*), Bmp and Wnt signaling (*Acvr1c*, *Bmpr2*, and *Amer1/2*), cell junction and polarity (*Nectin1*, *Cldn4*, *Dlgap3*, and *Pard3*), and cilia morphogenesis (*Alms1*, *Cep162*, *Rfx3*, and *Ulk4*) (Supplementary Fig. 5). In addition, common DRGs were for receptors (*Ffar1* and *Trpc1*), kinases (*Prkab2* and *Jak*), the phosphatidylinositol 3-kinase/AKT/FoxO1 signaling pathway (*Akt3*, *Insr*, and *Foxo1*), Ca^{2+} transport (*Trpc1* and *Grin2c*), and proteins involved in amino acid transport (*Slc7a11* and *Slc36a1*). A total of 114 long noncoding RNAs (lncRNAs) were also reduced in all three comparisons (Supplementary Fig. 6).

Analysis of genes that were dysregulated only in the presence of both stresses (1,098 URGs and 1,407 DRGs) (Fig. 6*A*) showed a further increase in oxidative phosphorylation, translation, and nucleotide metabolism genes and a decrease in microtubule-based processes, RNA transport, cilia, and nuclear pore organization genes (Supplementary Fig. 7 and Supplementary Table 5). Importantly, an increase in genes that impair glucose utilization for energy production (*Hmgcs2* and *Pdk4*) was observed only when excitotoxicity and overnutrition were combined, suggesting that the two stresses additively cause metabolic inflexibility.

Sex Influences the Responses to Excitotoxicity and Overnutrition

To determine how sex affects the response of β-cells to excitotoxicity and overnutrition, we reanalyzed our glucose homeostasis measurements and transcriptome data to extract these differences. As shown in Supplementary Figs. 8 and 9, male WT and KO mice gained more weight

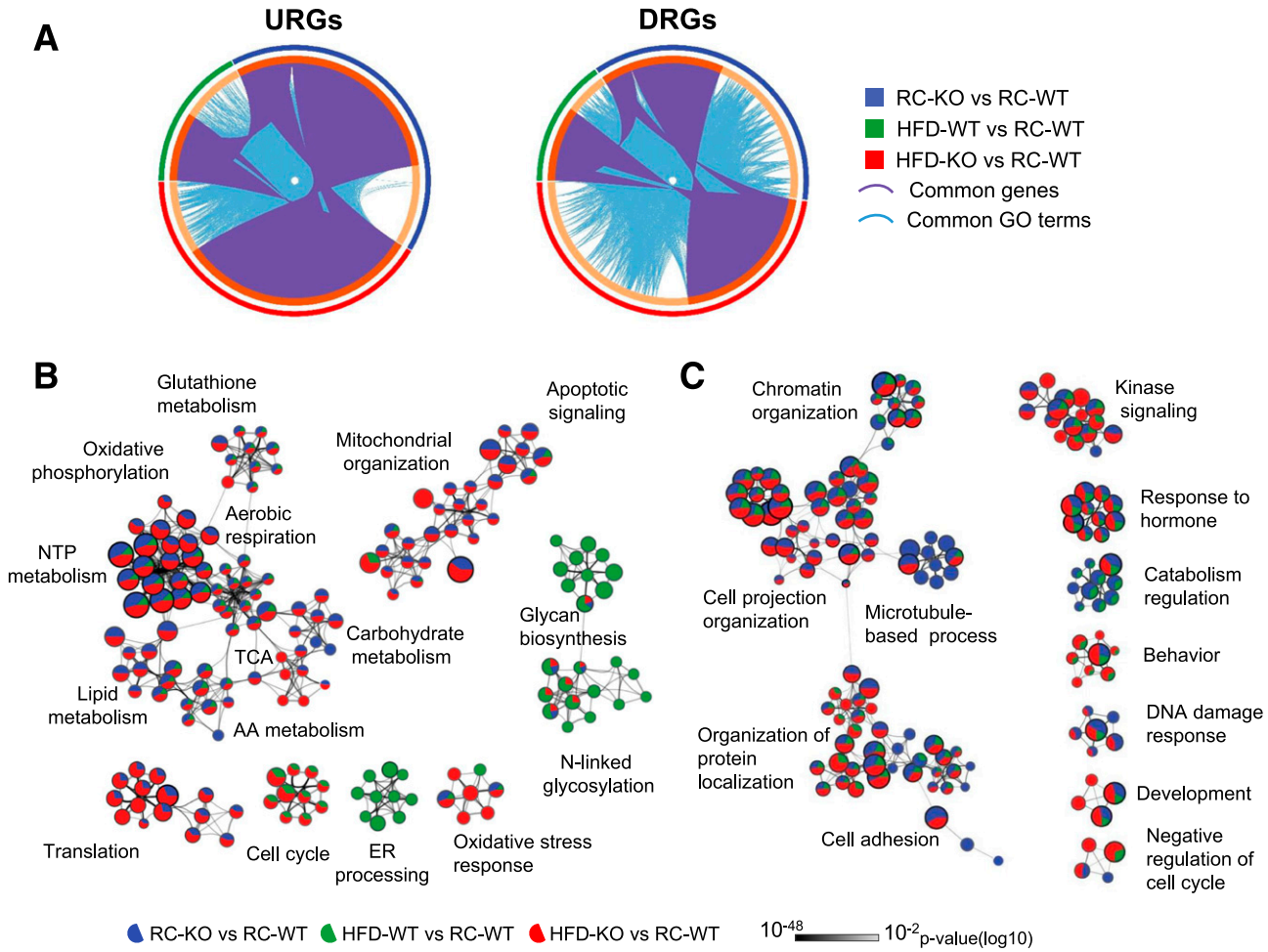

Figure 5—GO terms and pathways common for β-cell genes dysregulated in excitotoxicity, overnutrition, and the combination of both stresses. *A*: Cord diagrams show genes (purple curves) and GO terms/pathways (blue curves) shared among lists of URGs and DRGs from three comparisons. Excitotoxicity (blue, RC-KO vs. RC-WT comparison), overnutrition (green, HFD-WT vs. RC-WT comparison), and excitotoxicity and overnutrition (green, HFD-KO vs. RC-WT comparison). Enrichment network visualization of GO terms/pathways shared among URGs (*B*) and DRGs (*C*) from the three comparisons. Node size is proportional to the number of genes in GO category, with pie charts indicating a proportion of genes from each comparison. Intensity of a node border color indicates GO category enrichment *P* value (from 10^{-48} to 10^{-2}). AA, amino acid; TCA, tricarboxylic acid.

and had higher fed glucose concentrations and greater glucose intolerance than females of the same genotypes after 5 weeks on HFD. Verapamil treatment during HFD improved glucose tolerance in both the WT and KO males, but not in females of the same genotypes (Supplementary Fig. 9). However, while verapamil improved insulin tolerance in both the WT males and females, it had no effect on the KO mice (Supplementary Fig. 10). These findings indicate that male mice are more susceptible to negative effects of increased $[Ca^{2+}]_i$ than are female animals.

To determine how sex affects β-cell stress responses, we performed four different female-versus-male pairwise comparisons on the RNA-sequencing data sets (Supplementary Tables 3 and 4). Comparison of the RC-WT, RC-KO, and HFD-KO data sets in this manner yielded 140, 36, and 126 sex-specific genes, respectively ($P_{adj} < 0.05$) (Supplementary Table 3). The lower number of sex-specific changes in the RC-KO and HFD-KO mice, compared with the RC-WT mice, suggests that the marked perturbation of the β-cell transcriptome that occurs in *Abcc8* KO mice hinders the detection of sex-related differences. However, 2,618 were differentially expressed between female and male HFD-WT data sets. Overlaying all of the differentially expressed genes from the four pairwise comparisons revealed seven core sex-enriched genes, with *Xist*, *Fmo1*, and *Kdm6a* being female enriched and *Kdm5d*, *Uty*, *Eif2s3y*, and *Ddx3y* being male enriched (Supplementary Fig. 11*A*).

GO analysis of sex-enriched genes from HFD-WT comparison revealed that female-enriched pathways included oxidative phosphorylation, proteasome degradation, spliceosome, glutathione metabolism, and adrenergic signaling. Male-enriched pathways included ER to Golgi vesicle traffic, autophagy, and cell cycle (Supplementary Fig. 11*B* and Supplementary Table 5). Among the top genes expressed higher in females on HFD were neuropeptides (*Npy* and

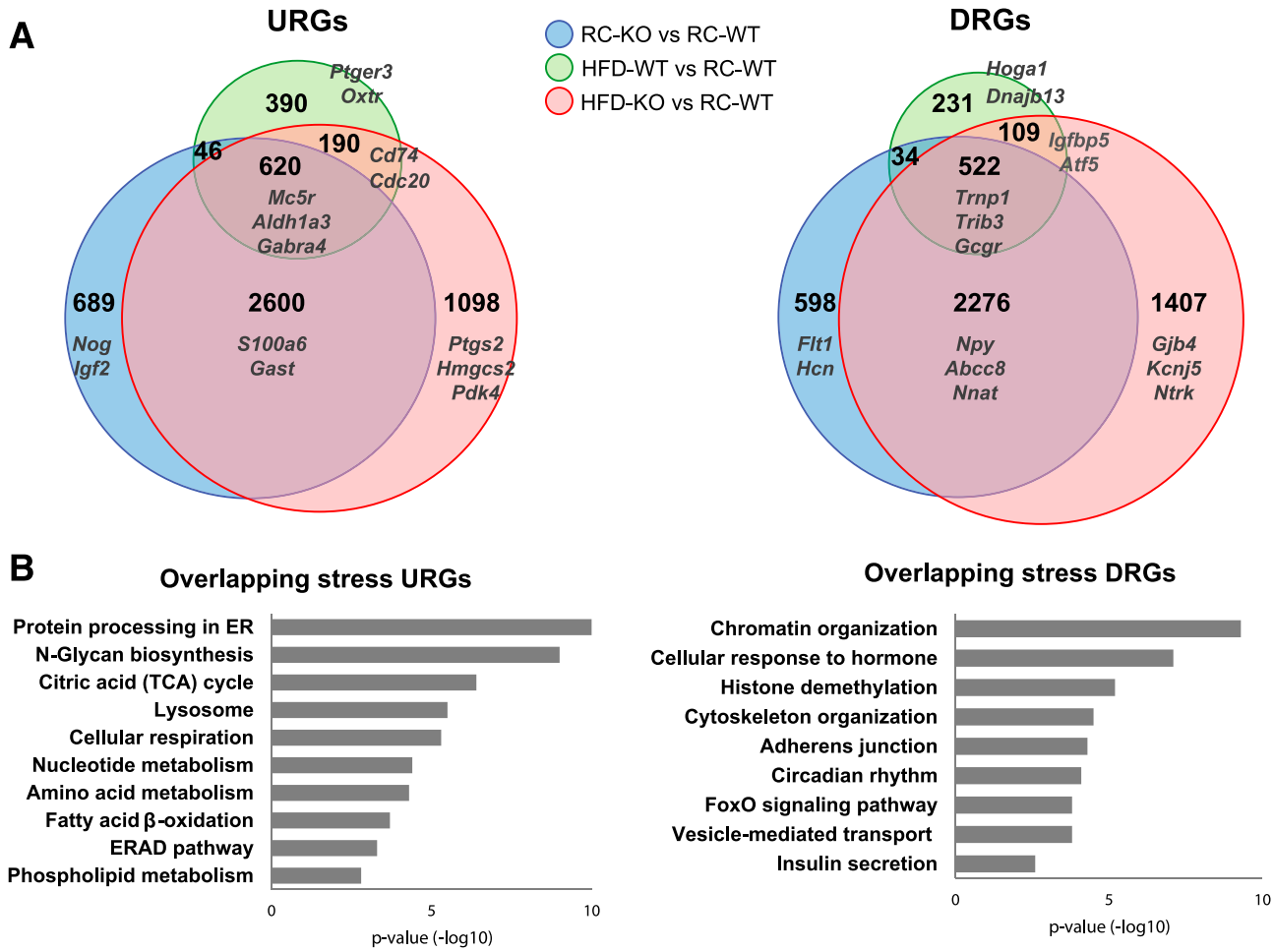

Figure 6—Overlapping β-cell genes dysregulated in excitotoxicity, overnutrition, and the combination of both stresses. *A*: Venn diagrams indicating overlap between DRGs or DRGs ($P_{adj} < 0.05$) identified from each pairwise comparison, with select top dysregulated genes indicated for each overlap. Excitotoxicity (blue, RC-KO vs. RC-WT comparison), overnutrition (light green, HFD-WT vs. RC-WT comparison), and excitotoxicity and overnutrition (pink, HFD-KO vs. RC-WT comparison). Genes in the circle that overlap among all three comparisons are overlapping stress URGs or DRGs. *B*: Functional enrichment analysis of URGs and DRGs. Select top enriched pathways are shown. ERAD, ER-associated protein degradation; TCA, tricarboxylic acid.

Pyy), hormones (*Gcg* and *Sst*), as well as developmental endocrine TFs (*Neurog3*, *Mafb*, *Fev*, *Arx*, and *Hhex*) (Supplementary Fig. 11*C*). In males, the more abundantly expressed genes included *Mc5r* and *Aldh1a3*, cell proliferation genes (*Mki76* and *Ccna*), DNA damage-response genes (*Pole* and *Fanca*), and transcriptional regulators (*Chd5*, *Bach2*, and *Txnip*). Overall, transcriptional response of male β-cells to HFD indicates a greater increase in β-cell proliferation, secretory function, autophagy, and associated DNA repair and ER-associated protein degradation pathways. The transcriptional response of female β-cells to HFD shows an increase in mitochondrial function, glutathione antioxidant defense, adrenergic signaling, and changes in β-cell identity.

Dysregulated Transcription Factor Gene Expression Is Modulated by Increased $[Ca^{2+}]_i$ and PA In Vitro

Because our in vivo analyses revealed the modulation of genes involved in mitochondrial energy production and the maintenance of β-cell identity, we further analyzed *Ppargc1a*, *Bach2*, *Thra*, and *Myt1* in cultured islets by RT-PCR (Fig. 7*A*). *Ppargc1a* is a transcriptional coregulator that is central to activation of mitochondrial energy metabolism, FA β-oxidation, and mitochondrial biogenesis (31). *Bach2* belongs to a family of TFs induced by oxidative stress that may play a role in immune-mediated β-cell apoptosis (32). *Myt1* and *Thra,* a thyroid hormone nuclear receptor, both contribute to the function of mature β-cells (33,34). Cultured WT mouse islets were treated with tolbutamide, a K_{ATP} channel inhibitor, PA, or a combination of both agents alone and with verapamil. After 24 h, the expression of *Ppargc1a* and *Bach2* was increased, and *Thra* and *Myt1* decreased, in response to tolbutamide alone. These changes were greatly accentuated when tolbutamide and PA were combined (Fig. 7*B*) and largely negated with the addition of verapamil. While the effect of PA by itself was generally small, its combination with tolbutamide was strongly additive, particularly for

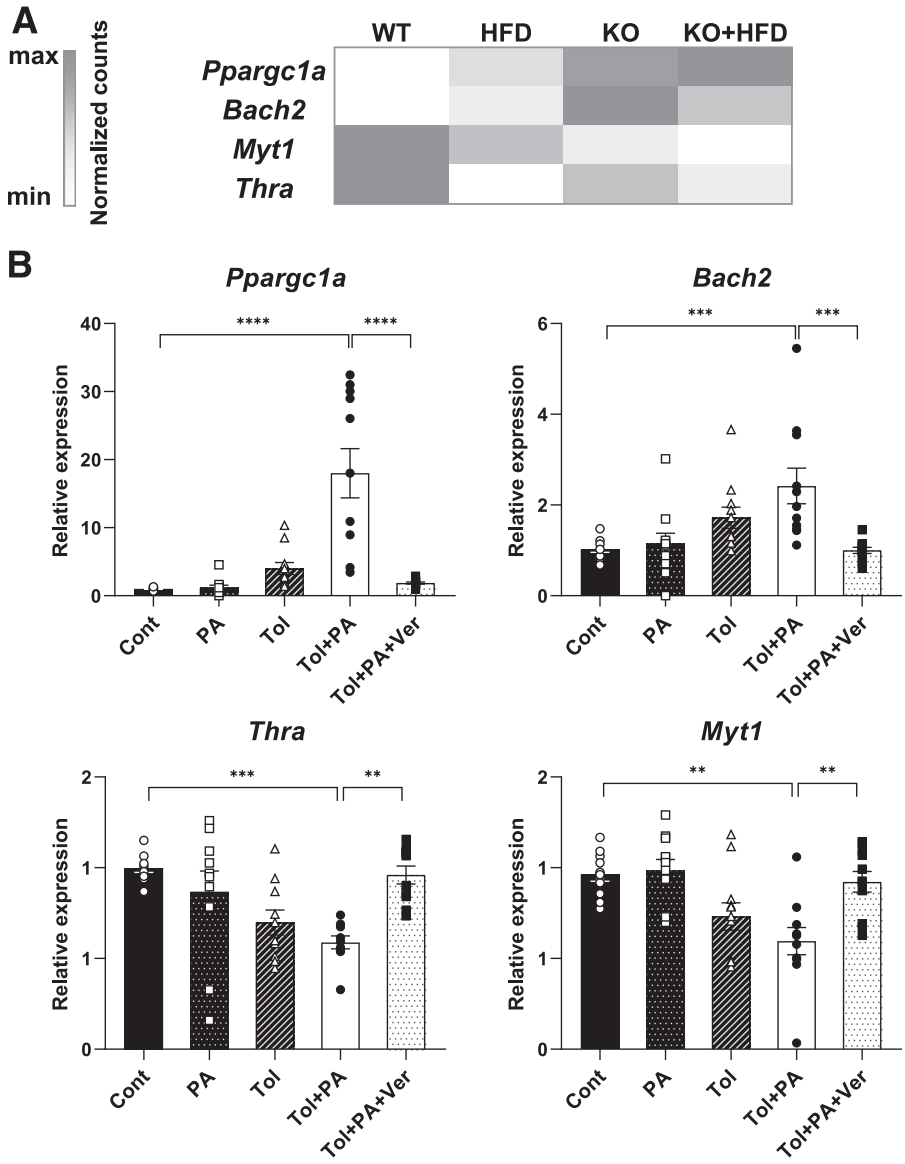

Figure 7—Expression of overlapping stress-dysregulated TFs is modulated by increased $[Ca^{2+}]_i$ and PA in vitro. *A*: Heat map of expression of TF genes *Ppargc1a*, *Bach2*, *Thra*, and *Myt1* in β-cells from RC-WT, HFD-WT, RC-KO, and HFD-KO mice. RNA-sequencing data were normalized across all data sets, with color intensity indicating relative gene expression level within each row. *B*: RT-qPCR results using whole-islet RNA from WT islets treated for 24 h with 100 μmol/L tolbutamide (Tol), 0.5 mmol/L PA, a combination of both (Tol+PA), and with 50 μmol/L verapamil (Tol+PA+Ver). Expression of *Ppargc1a* and *Bach2* is upregulated and expression of *Thra* and *Myt1* is downregulated in response to drug treatment, with the most pronounced effect occurring in response to PA. The effects are negated when Ca^{2+} influx is blocked with verapamil. Data from five experiments containing both male and female samples were averaged for a total of 10 different islet samples. Error bars: ± SEM. $^{**}P \leq 0.01$; $^{***}P \leq 0.001$; $^{****}P \leq 0.0001$ (determined by ANOVA). Cont, control; max, maximum; min, minimum.

Ppargc1a. These findings provide additional evidence for rapid changes in key β-cell TFs and FA signaling in response to a rise in $[Ca^{2+}]_i$.

Excitotoxicity and Overnutrition Additively Impair Mitochondrial Function

In β-cells, mitochondrial metabolism is essential for coupling glucose metabolism to insulin secretion. To determine whether the observed increases in genes involved in mitochondrial respiration, organization, and FA β-oxidation reflect actual changes in mitochondrial function, we compared mitochondrial OCR and mitochondrial biogenesis of RC-WT, RC-KO, HFD-WT, and HFD-KO islets. OCR measurements (Fig. 8*A*) showed that basal respiration rate reflecting the cell baseline metabolic energy production was progressively increased in HFD-WT, RC-KO, and HFD-KO islets (Fig. 8*B*). Similarly, metabolically stressed islets also had increased spare respiratory capacity, indicating increased ability to respond to increased energy demand (Fig. 8*C*) and increased mtDNA copy number (Fig. 8*F*). These results are consistent with corresponding increases in both mitochondrial respiration

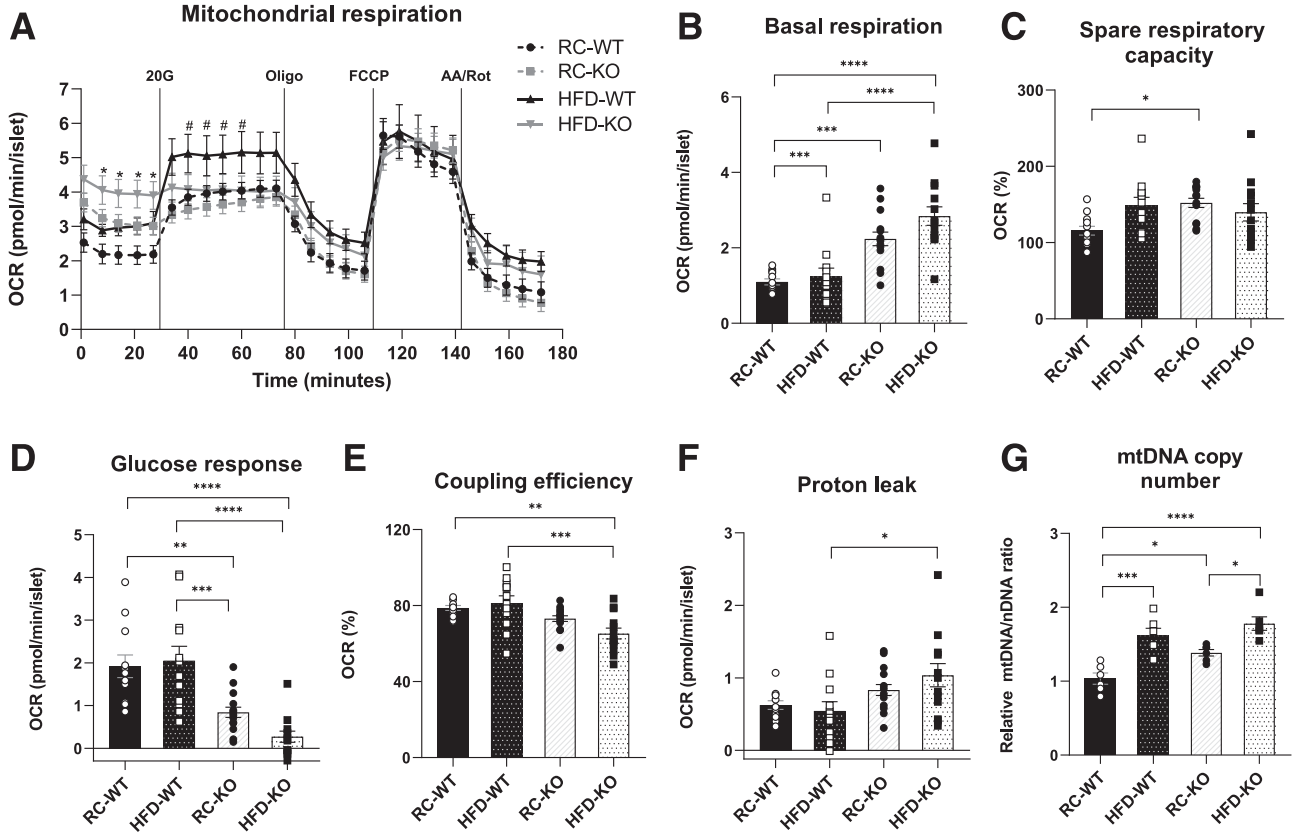

Figure 8—Excitotoxicity and overnutrition affect islet mitochondrial function. *A*: OCR profiles measured by Agilent Seahorse mitochondrial stress assay. Islets from RC-WT, HFD-WT, RC-KO, and HFD-KO male mice at 8–9 weeks of age were consecutively treated with 20 mmol/L glucose (20G), 5 mmol/L oligomycin A (Oligo), 1 mmol/L FCCP, and 2.5 mmol/L antimycin A/rotenone (AA/Rot). $n = 12$ wells for each condition. *$P \leq 0.05$, RC-WT vs. HFD-KO; #$P \leq 0.05$, RC-KO vs. HFD-WT. *B*: Basal respiration was increased in HFD-WT, RC-KO, and HFD-KO islets. Basal respiration rate was calculated by subtraction of nonmitochondrial respiration from basal respiration rate. *C*: Spare respiratory capacity, or the ratio of basal respiration to maximal respiration after FCCP injection (×100), was increased in RC-KO islets. *D*: Glucose-stimulated OCR response was decreased in RC-KO and HFD-KO islets. Glucose response was calculated by subtracting basal respiration rate from the OCR after glucose injection. *E*: Coupling efficiency, or the ratio of basal respiration to ATP production rate (×100), was decreased in HFD-KO islets. The ATP production rate was calculated by subtracting the minimal rate after oligomycin injection from the basal respiration rate. *F*: Proton leak, or the minimal rate after oligomycin injection minus nonmitochondrial respiration, was increased in RC-KO and HFD-KO islets. *G*: Relative mtDNA copy number was increased in HFD-WT, RC-KO, and HFD-KO islets. mtDNA to nuclear DNA (nDNA) using real-time PCR. Error bars: ± SEM. *$P \leq 0.05$; **$P \leq 0.01$; ***$P \leq 0.001$; ****$P \leq 0.0001$ (determined by ANOVA).

and biogenesis gene expression. However, the change in OCR in response to glucose is significantly decreased in RC-KO islets and almost completely ablated in HFD-KO islets (Fig. 8*D*), indicating that excitotoxicity and overnutrition additively impair mitochondrial glucose metabolism, most likely due to an increased FA β-oxidation, a rise in metabolic inflexibility, and mitochondrial damage. Consistent with an additive increase in mitochondrial damage, mitochondrial coupling efficiency is decreased and proton leak is increased in HFD-KO islets (Fig. 8*E* and *F*). These findings directly indicate that excitotoxicity and overnutrition additively impair mitochondrial glucose metabolic coupling function.

DISCUSSION

To gain a systems-wide understanding of pancreatic β-cell failure, we explored the additive effects of excitotoxicity and overnutrition on β-cell function and gene expression. Among the many changes that occur in β-cells in response to metabolic stress, we identified several critical alterations that may be tipping points for the development of T2D.

Excitotoxicity and HFD Additively Impair β-Cell Function

It has long been known that C57BL/6J (WT) mice develop insulin resistance and impaired β-cell function on an HFD (35). Our studies strongly suggest that an increase in $[Ca^{2+}]_i$, as occurs in the *Abcc8* KO β-cells, increases the propensity of β-cell to fail in response to HFD and, conversely, verapamil, which blocks calcium entry and protects against the loss of β-cell function. RC-KO mice, which are euglycemic at 8–9 weeks of age (11,23), exhibit greater insulin sensitivity than RC-WT mice, as has been reported for mice lacking *Kcnj11*, another essential K_{ATP} channel component (36). While HFD predictably caused insulin resistance in WT mice, *Abcc8* KO mice, like *Kcnj11*

KO animals (37), remained insulin sensitive on HFD, indicating that observed impairments in glucose homeostasis are mostly due to loss of β-cell function. Furthermore, while verapamil had no effect on insulin sensitivity in the KO mice, it increased the insulin sensitivity of WT mice on an HFD. Thus, our results not only confirm that Ca^{2+} channel blockers attenuate the development of obesity-induced insulin resistance (38), but they also indicate that the protective effects of these agents extend to β-cells. Moreover, they also indicate that an increase in $[Ca^{2+}]_i$, besides contributing to obesity-induced insulin resistance (39), has a negative effect on β-cell function. Indeed, given the pleiotropic metabolic effects of dysregulated Ca^{2+} homeostasis, it is noteworthy that the effects of Ca^{2+} channel blockers in both type 1 diabetes and T2D are now being investigated (40,41).

β-Cell Transcriptome Changes in Response to Excitotoxicity, HFD, and a Combination of Both Stresses

Excitotoxicity and overnutrition each have a major impact on β-cell gene expression, and together, the two stresses affect the expression of 11,952 unique genes, or nearly three-quarters (72%) of all genes expressed in β-cells. We also observed an overlap between genes and pathways that were dysregulated in response to both stresses, suggesting that increased $[Ca^{2+}]_i$ may be involved in mediating the nuclear responses of other metabolic stresses.

Energy Metabolism and Mitochondrial Function

The largest category of genes upregulated by excitotoxicity and/or overnutrition are those involved in mitochondrial function, metabolism, and oxidative phosphorylation. Mitochondrial metabolism is a major determinant of insulin secretion from pancreatic β-cells, and mitochondrial dysfunction plays a key role in development of T2D (42). Increased $[Ca^{2+}]_i$, in both normal and pathological states, invariably leads to increased mitochondrial Ca^{2+} uptake that stimulates mitochondrial Ca^{2+}-sensitive metabolic enzymes and oxidative phosphorylation in the electron transport chain (43). However, a persistent increase in mitochondrial $[Ca^{2+}]$ and respiration may lead to an increase in reactive oxygen species production, collapse of the mitochondrial membrane potential, and mitochondrial dysfunction (6). Consistently, we observed that even though mitochondrial biogenesis and basal respiration are increased in KO islets, they also exhibit decreased coupling efficiency and increased proton leak upon addition of HFD, indicating mounting mitochondrial damage. Normally, damaged mitochondria are replaced by the combination of mitophagy, a lysosomal-based degradation process, and the production of new mitochondria that occurs through mitochondrial biogenesis. A balance between these processes is essential for normal β-cell function (44). Excitotoxicity increases the expression of multiple mitochondrial and lysosomal genes, as well as master regulators of both mitochondrial (*Ppargc1a*) and lysosomal (*Tfeb*) biogeneses, potentially maintaining biogenesis/mitophagy balance. However, the combination of both excitotoxicity and overnutrition shifts this balance, as there is a further increase in mitochondrial energy metabolism, oxidative stress, and DNA damage-response genes, indicating an increase in reactive oxygen species and mitochondrial damage, while expression of lysosomal genes is not further changed, and several mitophagy-associated genes, such as *Clec16a* and *Prkn* (45), become downregulated. These results suggest that the combination of excitotoxicity and overnutrition overwhelms the ability of β-cells to replace metabolically damaged mitochondria.

Ppargc1a, a central transcriptional regulator of mitochondrial biogenesis, energy metabolism, and FA β-oxidation, is also increased in β-cells in response to both excitotoxicity and overnutrition. PPARGC1A interacts with multiple TFs and chromatin modifiers to regulate metabolic reprogramming in response to diet and oxidative stress and is implicated in pathogenesis of T2D (46). *Ppargc1a* is necessary for normal β-cell function (47), and its overexpression causes β-cell dysfunction (48). In this study, we show that expression of *Ppargc1a* is induced in cultured WT islets in response to increases in $[Ca^{2+}]_i$ and is further increased with the addition of PA. This finding further implicates $[Ca^{2+}]_i$ as an important regulator of mitochondrial metabolism in β-cells and suggests that an increase in $[Ca^{2+}]_i$ causes the rapid upregulation of *Ppargc1a*, most likely through the activation of Ca^{2+}-dependent CaN/CaMK/MAPK/AMPK signaling pathways. Similar signaling pathways are activated in skeletal muscle cells in response to exercise (49). In support of this hypothesis, excitotoxicity and overnutrition both upregulate *Mef2c*, a known target of Ca^{2+} signaling and a known activator of *Paprgc1a* in muscle, several CaMK and MAPKs, and multiple *Ppargc1a* target genes (Supplementary Fig. 12*A*). Similar to the activation of *Ppargc1a*, we also confirm an additive effect of increased $[Ca^{2+}]_i$ and PA on the upregulation of *Bach2*, an oxidative stress–responsive TF, and the downregulation of both *Myt1* and *Thra*, two other TFs important for the function of mature β-cells. However, less is known about how these other important genes are regulated and how they may contribute to normal β-cell function and the maintenance of β-cell identity.

Coupling of glucose metabolism to insulin secretion is an important aspect of mitochondrial function in β-cells. We find that the combination of excitotoxicity and overnutrition increases expression of genes that contribute to metabolic inflexibility or the decreased ability to use glucose as an energy source, another key feature of β-cell failure (50). Similar to overnutrition alone, excitotoxicity alone causes an increase in genes involved in FA β-oxidation, indicating that β-cells partially switch to utilization of fat as a fuel in response to an increased $[Ca^{2+}]_i$, a process known as glucose sparing (Supplementary Fig. 12*B*). This switch is reflected in reduced ability of KO islets to increase mitochondrial respiration in response to glucose. However, in addition to FA β-oxidation, combination of excitotoxicity

and overnutrition causes increases in *Pdk4*, a kinase that inhibits pyruvate flux into the tricarboxylic acid cycle, promoting FA and ketone body utilization (51), and *Hmgcs2*, a rate-limiting enzyme in ketone body production that is activated by FAs (52). Because these changes would be expected to impair glycolytic flux and cause metabolic inflexibility (Supplementary Fig. 12*C*), they may explain the observed collapse of mitochondrial glucose response in HFD-KO islets. Therefore, our data suggest a tipping point at which the combination of an increase in $[Ca^{2+}]_i$ and an elevation in FAs causes the β-cell to cease relying on glycolysis and to switch to FAs and ketones as their fuel source, impairing their ability to sense and respond to changes in the blood glucose concentration.

ER Protein Folding and Protein Glycosylation

Glycosylation is a process during which glycans (mono- or oligosaccharides) are attached to proteins in the ER and Golgi that serve as a quality control signal in ER protein folding (53). In β-cells, increases in protein glycosylation cause ER stress, eventually leading to apoptosis (54). We found that overnutrition in particular increased expression of genes associated with ER protein folding and *N*- and *O*-linked protein glycosylation, suggesting that the stability, localization, trafficking, and function of many receptors, ion channels, nutrient transporters, and TFs are also adversely affected, likely contributing to development of T2D (55).

β-Cell Structure: Cytoskeleton, Cell Polarity, and Cell Adhesion

Excitotoxicity, overnutrition, and the combination of both stresses downregulate genes important for cell organization and secretory function of β-cells, including cell adhesion, cell junctions, cilia, cytoskeleton, and vesicular trafficking genes. We have previously identified impairments in islet architecture of *Abcc8* KO mice (11), suggesting that critical cell-to-cell contacts, which are necessary for insulin secretion, may become impaired (56). The downregulation of synaptic vesicle-targeting proteins, GTPases, and cytoskeletal proteins has been shown to affect insulin exocytosis (57). Similarly, alterations in β-cell polarity may occur as genes associated with the apical domain (*Pard3*) and associated primary cilia (*Alms1* and *Cep162*) and lateral domain (*Dlgap3* and *Nectin1*) are downregulated, and genes associated with the vasculature-facing basal domain (*Col8a2*, *Ntn4*, and *Ppfia3*) are increased (58). These changes indicate that Ca^{2+} signaling in β-cells is crucial for maintaining cell polarity and cytoskeleton dynamics and that a chronic increase in $[Ca^{2+}]_i$ impairs the ability of these cells to secrete insulin.

β-Cell Identity

Another important category of genes downregulated in metabolically stressed β-cells is those involved in transcriptional control. Besides decreases in many TFs that are necessary for function of mature β-cells (*Myt1*, *Thra*, *Pbx1*, *Stat5a*, and *Nrf1*), we also identified several other stress-inhibited TFs (*Mesp2*, *Klf7*, *Nfia*, *Ikzf3*, and *Chd7*) that may be critical for maintaining β-cell identity and function. Similarly, many chromatin modifiers, including histone methyltransferases and acetyltransferases, were downregulated in response to both stresses. Among these is *Dnmt3a*, a DNA methyltransferase important for silencing of developmental or "disallowed" metabolic genes in mature β-cells (59). Consistent with this, several disallowed genes (60) (*Slc16a*, *Oat*, and *Aldob*) are upregulated in response to excitotoxicity and/or overnutrition. Finally, maintenance of the epigenetic and transcriptional landscape of β-cells is also regulated by lncRNAs (61), and we identified multiple lncRNAs that are downregulated in response to these two metabolic stresses.

Effects of Sex on β-Cell Stress Responses

Male rodents have a greater propensity for β-cell failure than do females (18). In this study, we analyzed the effects of excitotoxicity and/or HFD on β-cell function and gene expression in both sexes. We found that female animals (both WT and *Abcc8* KOs) withstand overnutrition better than males. These results are consistent with previous data on HFD-WT mice (62) and may reflect the protective influence of female sex hormones on β-cell function and metabolism (63). Interestingly, verapamil improved insulin sensitivity and glucose clearance in both the HFD-WT and HFD-KO males, but had little effect in females, suggesting that males are more negatively affected by a stress-induced increase in $[Ca^{2+}]_i$ than females. Testosterone is known to increase $[Ca^{2+}]_i$ in multiple tissues (64) and may also predispose β-cells for dysfunction associated with further $[Ca^{2+}]_i$ increase due to increased metabolic load.

Analysis of sex differences on a transcriptome level in WT mice confirmed our previous findings that female β-cells express higher amounts of several TFs important for β-cell function including *Mlxipl*, *Nkx2-2*, and *Hnf1b* (22). Interestingly, we were only able to detect a few sex-related changes in β-cells from both RC- and HFD-*Abcc8* KO mice, suggesting that the massive gene expression changes that occur in the *Abcc8* KO mice may mask the detection of sex-related differences. However, overlaying the differentially expressed genes from all four female to male transcriptome comparisons allowed us to identify three core female-enriched β-cell genes (*Xist*, *Fmo1*, and *Kdm6a*) and four male-enriched genes (*Kdm5d*, *Uty*, *Eif2s3y*, and *Ddx3y*). All of the male-enriched genes are located on the Y chromosome, whereas only two of the female-enriched genes (*Xist* and *Kdm6a*) are located on the X chromosome. *Kdm6a*, *Uty*, and *Kdm5d* all code for histone demethylases that may be involved in sex-specific epigenetic regulation of gene expression (65,66). Our discovery that *Fmo1*, an autosome-located gene, is enriched in female β-cells is interesting, as this gene encodes a flavin-containing monooxgenase 1, a drug-metabolizing enzyme that regulates energy balance (67). Another member of the same family, *Fmo4*, was also upregulated in

females on HFD. Overall, the most profound sex differences revealed by our analysis were in the β-cell transcriptome on HFD (2,618 genes). Female β-cells express higher levels of genes involved in oxidative phosphorylation, suggesting they may have higher energy metabolism than do male β-cells. Genes involved in prevention of oxidative damage, such as glutathione peroxidases, are also higher in female cells, suggesting a mechanism enabling female β-cells to tolerate overnutrition better than males. Female β-cells also express more of neuropeptides *Npy* and *Pyy*, both of which could be protective against β-cell damage (68,69), and the adrenergic receptor *Adrb2*, signaling through which can increase insulin secretion. Consistent with this, it was recently reported that pancreas-specific loss of *Adrb2* causes glucose intolerance and impaired glucose-stimulated insulin secretion only in female mice (70). Intriguingly, genes associated with endocrine progenitor (*Neurog3* and *Mafb*) and α-cells (*Gcg* and *Arx*) and δ-cells (*Sst* and *Hhex*) are upregulated in HFD-fed female β-cells, suggesting changes in cell identity. Male mice fed HFD exhibit higher expression of β-cell genes involved in protein secretion and cell proliferation, consistent with the well-established fact that male β-cells exhibit greater proliferation when fed HFD (71).

Concluding Remarks

We have identified many different genes and pathways in β-cells that are affected by metabolic stress. The broad-based nature of the changes we observe suggests that β-cell failure in T2D is not due to the failure of a single cellular process, but instead is a complex, multifaceted, and additive process in which Ca^{2+} signaling plays a crucial role.

Acknowledgments. The authors thank the Vanderbilt Technologies for Advanced Genomics (VANTAGE) Core and the Vanderbilt University Medical Center Flow Cytometry Shared Resource for assistance in performing cell sorting and RNA sequencing and the Vanderbilt Islet Procurement and Analysis Core for help with isolating islets.

Funding. This research was supported by institutional and philanthropic funds provided by Vanderbilt University. The Vanderbilt Islet Procurement and Analysis Core is supported by DK-020593. VANTAGE is supported by grants P30-CA-68485, P30-EY-08126, and G20-RR-030956. Vanderbilt University Medical Center Flow Cytometry Shared Resource is supported by grants P30-CA-68485 and DK-058404.

Duality of Interest. No potential conflicts of interest relevant to this article were reported.

Author Contributions. A.B.O. and M.A.M. designed the study. A.B.O., J.S.S., and K.D.D. performed experiments. A.B.O. analyzed the data. J.-P.C. performed RNA-sequencing data processing, alignment, and DE analyses. A.B.O. and M.A.M. wrote and edited the manuscript. J.S.S. edited the manuscript. M.A.M. is the guarantor of this work and, as such, had full access to all the data in the study and takes responsibility for the integrity of the data and the accuracy of the data analysis.

References

1. Halban PA, Polonsky KS, Bowden DW, et al. β-Cell failure in type 2 diabetes: postulated mechanisms and prospects for prevention and treatment. Diabetes Care 2014;37:1751–1758

2. Poitout V, Amyot J, Semache M, Zarrouki B, Hagman D, Fontés G. Glucolipotoxicity of the pancreatic beta cell. Biochim Biophys Acta 2010;1801:289–298

3. Grill V, Björklund A. Overstimulation and beta-cell function. Diabetes 2001; 50(Suppl. 1):S122–S124

4. Hasnain SZ, Prins JB, McGuckin MA. Oxidative and endoplasmic reticulum stress in β-cell dysfunction in diabetes. J Mol Endocrinol 2016;56:R33–R54

5. Böni-Schnetzler M, Meier DT. Islet inflammation in type 2 diabetes. Semin Immunopathol 2019;41:501–513

6. Bano D, Ankarcrona M. Beyond the critical point: an overview of excitotoxicity, calcium overload and the downstream consequences. Neurosci Lett 2018;663:79–85

7. Sabatini PV, Speckmann T, Lynn FC. Friend and foe: β-cell Ca^{2+} signaling and the development of diabetes. Mol Metab 2019;21:1–12

8. Khaldi MZ, Guiot Y, Gilon P, Henquin JC, Jonas JC. Increased glucose sensitivity of both triggering and amplifying pathways of insulin secretion in rat islets cultured for 1 wk in high glucose. Am J Physiol Endocrinol Metab 2004;287: E207–E217

9. Do OH, Low JT, Gaisano HY, Thorn P. The secretory deficit in islets from db/db mice is mainly due to a loss of responding beta cells. Diabetologia 2014;57:1400–1409

10. Chen C, Chmelova H, Cohrs CM, et al. Alterations in β-cell calcium dynamics and efficacy outweigh islet mass adaptation in compensation of insulin resistance and prediabetes onset. Diabetes 2016;65:2676–2685

11. Stancill JS, Cartailler JP, Clayton HW, et al. Chronic β-cell depolarization impairs β-cell identity by disrupting a network of Ca^{2+}-regulated genes. Diabetes 2017;66:2175–2187

12. Xu G, Chen J, Jing G, Shalev A. Preventing β-cell loss and diabetes with calcium channel blockers. Diabetes 2012;61:848–856

13. Lee K, Kim J, Köhler M, et al. Blocking Ca^{2+} channel β_3 subunit reverses diabetes. Cell Rep 2018;24:922–934

14. Imai Y, Cousins RS, Liu S, Phelps BM, Promes JA. Connecting pancreatic islet lipid metabolism with insulin secretion and the development of type 2 diabetes. Ann N Y Acad Sci 2020;1461:53–72

15. Cnop M, Ladrière L, Igoillo-Esteve M, Moura RF, Cunha DA. Causes and cures for endoplasmic reticulum stress in lipotoxic β-cell dysfunction. Diabetes Obes Metab 2010;12(Suppl. 2):76–82

16. Keane KN, Cruzat VF, Carlessi R, de Bittencourt PI Jr., Newsholme P. Molecular events linking oxidative stress and inflammation to insulin resistance and β-cell dysfunction. Oxid Med Cell Longev 2015;2015:181643

17. Hara T, Mahadevan J, Kanekura K, Hara M, Lu S, Urano F. Calcium efflux from the endoplasmic reticulum leads to β-cell death. Endocrinology 2014;155: 758–768

18. Gannon M, Kulkarni RN, Tse HM, Mauvais-Jarvis F. Sex differences underlying pancreatic islet biology and its dysfunction. Mol Metab 2018;15:82–91

19. Kautzky-Willer A, Harreiter J, Pacini G. Sex and gender differences in risk, pathophysiology and complications of type 2 diabetes mellitus. Endocr Rev 2016; 37:278–316

20. Tiano JP, Delghingaro-Augusto V, Le May C, et al. Estrogen receptor activation reduces lipid synthesis in pancreatic islets and prevents β cell failure in rodent models of type 2 diabetes. J Clin Invest 2011;121:3331–3342

21. Hall E, Volkov P, Dayeh T, et al. Sex differences in the genome-wide DNA methylation pattern and impact on gene expression, microRNA levels and insulin secretion in human pancreatic islets. Genome Biol 2014;15:522

22. Stancill JS, Osipovich AB, Cartailler JP, Magnuson MA. Transgene-associated human growth hormone expression in pancreatic β-cells impairs identification of sex-based gene expression differences. Am J Physiol Endocrinol Metab 2019;316: E196–E209

23. Shiota C, Larsson O, Shelton KD, et al. Sulfonylurea receptor type 1 knock-out mice have intact feeding-stimulated insulin secretion despite marked impairment in their response to glucose. J Biol Chem 2002;277:37176–37183

24. Taddeo EP, Stiles L, Sereda S, et al. Individual islet respirometry reveals functional diversity within the islet population of mice and human donors. Mol Metab 2018;16:150–159

25. Shiota C, Rocheleau JV, Shiota M, Piston DW, Magnuson MA. Impaired glucagon secretory responses in mice lacking the type 1 sulfonylurea receptor. Am J Physiol Endocrinol Metab 2005;289:E570–E577
26. Dahan T, Ziv O, Horwitz E, et al. Pancreatic β-cells express the fetal islet hormone gastrin in rodent and human diabetes. Diabetes 2017;66:426–436
27. Kim-Muller JY, Fan J, Kim YJ, et al. Aldehyde dehydrogenase 1a3 defines a subset of failing pancreatic β cells in diabetic mice. Nat Commun 2016;7:12631
28. Soltani N, Qiu H, Aleksic M, et al. GABA exerts protective and regenerative effects on islet beta cells and reverses diabetes. Proc Natl Acad Sci U S A 2011; 108:11692–11697
29. Volpe M, Shpungin S, Barbi C, et al. trnp: a conserved mammalian gene encoding a nuclear protein that accelerates cell-cycle progression. DNA Cell Biol 2006;25:331–339
30. Mondal D, Mathur A, Chandra PK. Tripping on TRIB3 at the junction of health, metabolic dysfunction and cancer. Biochimie 2016;124:34–52
31. Austin S, St-Pierre J. PGC1α and mitochondrial metabolism–emerging concepts and relevance in ageing and neurodegenerative disorders. J Cell Sci 2012;125:4963–4971
32. Marroquí L, Santin I, Dos Santos RS, Marselli L, Marchetti P, Eizirik DL. BACH2, a candidate risk gene for type 1 diabetes, regulates apoptosis in pancreatic β-cells via JNK1 modulation and crosstalk with the candidate gene PTPN2. Diabetes 2014;63:2516–2527
33. Aguayo-Mazzucato C, Zavacki AM, Marinelarena A, et al. Thyroid hormone promotes postnatal rat pancreatic β-cell development and glucose-responsive insulin secretion through MAFA. Diabetes 2013;62:1569–1580
34. Wang S, Zhang J, Zhao A, Hipkens S, Magnuson MA, Gu G. Loss of Myt1 function partially compromises endocrine islet cell differentiation and pancreatic physiological function in the mouse. Mech Dev 2007;124:898–910
35. Nicholson A, Reifsnyder PC, Malcolm RD, et al. Diet-induced obesity in two C57BL/6 substrains with intact or mutant nicotinamide nucleotide transhydrogenase (Nnt) gene. Obesity (Silver Spring) 2010;18:1902–1905
36. Miki T, Nagashima K, Tashiro F, et al. Defective insulin secretion and enhanced insulin action in KATP channel-deficient mice. Proc Natl Acad Sci U S A 1998;95:10402–10406
37. Remedi MS, Koster JC, Markova K, et al. Diet-induced glucose intolerance in mice with decreased beta-cell ATP-sensitive K+ channels. Diabetes 2004;53:3159–3167
38. Kim JH, Mynatt RL, Moore JW, Woychik RP, Moustaid N, Zemel MB. The effects of calcium channel blockade on agouti-induced obesity. FASEB J 1996;10: 1646–1652
39. Kang JK, Kim OH, Hur J, et al. Increased intracellular Ca^{2+} concentrations prevent membrane localization of PH domains through the formation of Ca^{2+}-phosphoinositides. Proc Natl Acad Sci U S A 2017;114:11926–11931
40. Carvalho DS, de Almeida AA, Borges AF, Vannucci Campos D. Treatments for diabetes mellitus type II: new perspectives regarding the possible role of calcium and cAMP interaction. Eur J Pharmacol 2018;830:9–16
41. Ovalle F, Grimes T, Xu G, et al. Verapamil and beta cell function in adults with recent-onset type 1 diabetes. Nat Med 2018;24:1108–1112
42. Yaribeygi H, Atkin SL, Sahebkar A. Mitochondrial dysfunction in diabetes and the regulatory roles of antidiabetic agents on the mitochondrial function. J Cell Physiol 2019;234:8402–8410
43. Wiederkehr A, Wollheim CB. Mitochondrial signals drive insulin secretion in the pancreatic β-cell. Mol Cell Endocrinol 2012;353:128–137
44. Rovira-Llopis S, Bañuls C, Diaz-Morales N, Hernandez-Mijares A, Rocha M, Victor VM. Mitochondrial dynamics in type 2 diabetes: pathophysiological implications. Redox Biol 2017;11:637–645
45. Kaufman BA, Li C, Soleimanpour SA. Mitochondrial regulation of β-cell function: maintaining the momentum for insulin release. Mol Aspects Med 2015;42:91–104
46. Besseiche A, Riveline JP, Gautier JF, Bréant B, Blondeau B. Metabolic roles of PGC-1α and its implications for type 2 diabetes. Diabetes Metab 2015;41:347–357
47. Oropeza D, Jouvet N, Bouyakdan K, et al. PGC-1 coactivators in β-cells regulate lipid metabolism and are essential for insulin secretion coupled to fatty acids. Mol Metab 2015;4:811–822
48. Besseiche A, Riveline JP, Delavallée L, Foufelle F, Gautier JF, Blondeau B. Oxidative and energetic stresses mediate beta-cell dysfunction induced by PGC-1α. Diabetes Metab 2018;44:45–54
49. Lira VA, Benton CR, Yan Z, Bonen A. PGC-1alpha regulation by exercise training and its influences on muscle function and insulin sensitivity. Am J Physiol Endocrinol Metab 2010;299:E145–E161
50. Kim-Muller JY, Zhao S, Srivastava S, et al. Metabolic inflexibility impairs insulin secretion and results in MODY-like diabetes in triple FoxO-deficient mice. Cell Metab 2014;20:593–602
51. Zhang S, Hulver MW, McMillan RP, Cline MA, Gilbert ER. The pivotal role of pyruvate dehydrogenase kinases in metabolic flexibility. Nutr Metab (Lond) 2014;11:10
52. Rescigno T, Capasso A, Tecce MF. Involvement of nutrients and nutritional mediators in mitochondrial 3-hydroxy-3-methylglutaryl-CoA synthase gene expression. J Cell Physiol 2018;233:3306–3314
53. Wang Q, Groenendyk J, Michalak M. Glycoprotein quality control and endoplasmic reticulum stress. Molecules 2015;20:13689–13704
54. Liu K, Paterson AJ, Chin E, Kudlow JE. Glucose stimulates protein modification by O-linked GlcNAc in pancreatic beta cells: linkage of O-linked GlcNAc to beta cell death. Proc Natl Acad Sci U S A 2000;97:2820–2825
55. Hart GW. Nutrient regulation of signaling and transcription. J Biol Chem 2019; 294:2211–2231
56. Dissanayake WC, Sorrenson B, Shepherd PR. The role of adherens junction proteins in the regulation of insulin secretion. Biosci Rep 2018;38:BSR20170989
57. Wang Z, Thurmond DC. Mechanisms of biphasic insulin-granule exocytosis - roles of the cytoskeleton, small GTPases and SNARE proteins. J Cell Sci 2009;122:893–903
58. Gan WJ, Zavortink M, Ludick C, et al. Cell polarity defines three distinct domains in pancreatic β-cells. J Cell Sci 2017;130:143–151
59. Dhawan S, Tschen SI, Zeng C, et al. DNA methylation directs functional maturation of pancreatic β cells. J Clin Invest 2015;125:2851–2860
60. Pullen TJ, Rutter GA. When less is more: the forbidden fruits of gene repression in the adult β-cell. Diabetes Obes Metab 2013;15:503–512
61. Esguerra JL, Eliasson L. Functional implications of long non-coding RNAs in the pancreatic islets of Langerhans. Front Genet 2014;5:209
62. Oliveira RB, Maschio DA, Carvalho CP, Collares-Buzato CB. Influence of gender and time diet exposure on endocrine pancreas remodeling in response to high fat diet-induced metabolic disturbances in mice. Ann Anat 2015;200:88–97
63. Mauvais-Jarvis F. Role of sex steroids in β cell function, growth, and survival. Trends Endocrinol Metab 2016;27:844–855
64. Vicencio JM, Estrada M, Galvis D, et al. Anabolic androgenic steroids and intracellular calcium signaling: a mini review on mechanisms and physiological implications. Mini Rev Med Chem 2011;11:390–398
65. Mizukami H, Kim JD, Tabara S, et al. KDM5D-mediated H3K4 demethylation is required for sexually dimorphic gene expression in mouse embryonic fibroblasts. J Biochem 2019;165:335–342
66. Gažová I, Lengeling A, Summers KM. Lysine demethylases KDM6A and UTY: the X and Y of histone demethylation. Mol Genet Metab 2019;127:31–44
67. Veeravalli S, Omar BA, Houseman L, et al. The phenotype of a flavin-containing monooyxgenase knockout mouse implicates the drug-metabolizing enzyme FMO1 as a novel regulator of energy balance. Biochem Pharmacol 2014;90:88–95
68. Khan D, Vasu S, Moffett RC, Irwin N, Flatt PR. Islet distribution of peptide YY and its regulatory role in primary mouse islets and immortalised rodent and human beta-cell function and survival. Mol Cell Endocrinol 2016;436:102–113
69. Khan D, Vasu S, Moffett RC, Irwin N, Flatt PR. Influence of neuropeptide Y and pancreatic polypeptide on islet function and beta-cell survival. Biochim Biophys Acta Gen Subj 2017;1861:749–758
70. Ceasrine AM, Lin EE, Lumelsky DN, Iyer R, Kuruvilla R. Adrb2 controls glucose homeostasis by developmental regulation of pancreatic islet vasculature. eLife 2018;7:e39689
71. Stamateris RE, Sharma RB, Hollern DA, Alonso LC. Adaptive β-cell proliferation increases early in high-fat feeding in mice, concurrent with metabolic changes, with induction of islet cyclin D2 expression. Am J Physiol Endocrinol Metab 2013;305:E149–E159